Study of the Mechanical, Thermal and Electronic Properties of Nanoscale Materials

K. Masuda-Jindo[1], Vu Van Hung[2] and M. Menon[3]

1 Department of Materials Science and Engineering, Tokyo Institute of Technology, Nagatsuta, Midori-ku, Yokohama 226-8503, Japan
kmjindo@issp.u-tokyo.ac.jp

2 Hanoi National Pedagogic University, km8 Hanoi-Sontay Highway, Hanoi, Vietnam

3 Department of Physics and Astronomy, University of Kentucky, Lexington, Kentucky 40506, U.S.A.

Abstract

The mechanical, thermal and electronic properties of the nanoscale materials are studied using an ab initio molecular dynamics (TBMD) method and statistical moment method (SMM). We investigate the strength and fracture behaviors of nanoscale materials like carbon nanotubes (CNT), graphens and nanowires in comparison with those of corresponding bulk materials. The thermal expansion coefficients, linear elastic parameters, nonlinear elastic instabilities, yield strength and fracture behaviors are studied including the anharmonicity of thermal vibrations. We will show that the thermodynamic and strength properties of the nanoscale materials are quite different from those of the corresponding bulk materials. The electronic density of states and electronic transports of the nanoscale materials, with and without the atomistic defects are also discussed.

Key words: carbon nanotube, mechanical property, quantum transport, thermodynamic property, SW defect

1. INTRODUCTION

Recently, there has been a great interest in the study of nanoscale materials since they provide us a wide variety of academic problems as well as the technological applications [1-6]. In particular, the discovery of carbon nanotubes (CNT) by Iijima [5] and subsequent observations of CNT's unique electronic and mechanical properties have initiated intensive research on these quasi-one-dimensional (1D) structures. Now, it has been observed that the introduction of lattice defects and mechanical deformation influence quite significantly on the electronical properties of nanoscale materials [7,8]. CNT's have been thus identified as one of the most promising building blocks for future development of functional nanostructures.

The purpose of the present paper is to investigate the strength and fracture behaviors of nanoscale materials using the ab initio tight-binding molecular dynamics method [9,10] combined with the temperature Lattice Green's function method [11-22]. We calculate the atomic configurations and strength properties of nanoscale materials including extended defects using the new version of the molecular dynamics method, constraint molecular dynamics (c-MD) method, on the basis of the analysis of the Lattice Green's function theory.

In the present study, we shall also study the thermodynamic and electronic properties of nanoscale materials including the temperature dependence of the atomistic spacing and the resulting changes in the interatomic force constants. We use the statistical moment method (SMM) [23-25], going beyond the quasi-harmonic approximation and apply the formalism to the fracture problem.

2. PRINCIPLE OF CALCULATIONS

For treating mechanical and thermodynamic properties of nanoscale materials we will use the ab initio tight-binding molecular dynamics methods [7,8], which have been very successful in the calculations of various chemical and physical properties of nanoscale materials. In the present article, we also use the constraint MD method combined with the lattice Green's function (LGF) approach to study the initiation of microcracks in the nanoscale materials, like graphen sheets, nanographites and nanotubes. In the treatment of LGF, we generalize the conventional LGF theory to take into account the temperature effects by including the temperature dependence of force constant matrices and non-linear cohesive forces.

2.1. Lattice Green's Function Method

In this subsection, we will briefly outline the essence of the lattice Green's function (LGF) method for the study of fracture (cracks) of the nano materials. In the LGF treatments, the so-called bond annihilation operations play an important roles in the crack initiation and opening processes of the "double" ended cracks. In the use of the mathematical terminology, the bond annihilation operators correspond to the "perturbation potential" V in the Dyson equation:

$$G = G_0 + G_0 V G, \qquad (1)$$

where G_0 and G represent the unperturbed and perturbed Green's functions, respectively. We will combine the concepts of the conventional LGF method with the numerical analysis by the molecular dynamics method to get the "equilibrium" crack geometries under the external loadings. We will call this combined

scheme the constraint MD method (c-MD). Following the c-MD scheme, the atomic bonds across the cleavage plane are annihilated at the initial stage of the MD simulation, but after the sufficient MD simulations, no assumptions on the bond breakings across the cleavage plane are made. Therefore, this type of constraint MD calculations, composed of two stage calculations, are expected to give an essentially identical results with those by the LGF method.

2.2. Statistical Moment Method (SMM)

Following the general procedure of the statistical moment method (SMM), we derive the thermodynamic quantities of nanoscale materials analytically, taking into account the higher (fourth) order anharmonic contributions in the thermal lattice vibrations going beyond the Quasi-Harmonic (QH) approximation. The basic equations for obtaining thermodynamic quantities are derived in a following manner: The equilibrium thermal lattice expansions are calculated by the force balance criterion and then the thermodynamic quantities are determined for the equilibrium lattice spacings. The anharmonic contributions of the thermodynamic quantities are given explicitly in terms of the power moments of the thermal atomic displacements. For the evaluation of the anharmonic contributions to the Free energy Ψ, we consider a quantum system, which is influenced by supplemental forces α_i in the space of the generalized coordinates q_i. For simplicity, we only discuss monatomic systems, and the Hamiltonian of the system is given by

$$\hat{H} = \hat{H}_0 - \sum_i \alpha_i \hat{q}_i, \qquad (2)$$

where $\hat{H}_0$ denotes the unperturbed Hamiltonian without the supplementary forces α_i and upper huts $\wedge$ represent operators. The supplementary forces α_i are acted in the direction of the generalized coordinates q_i. The thermodynamic quantities of the harmonic approximation (harmonic Hamiltonian) will be treated in the Einstein model.

Once the thermal expansion Δr in the given system is found, one can get the Helmholtz free energy of the system in the following form

$$\Psi = U_0 + \Psi_0 + \Psi_1, \qquad (3)$$

where Ψ_0 denotes the free energy in the harmonic approximation and Ψ_1 the anharmonicity contribution to the free energy. We calculate the anharmonicity contribution to the free energy Ψ_1 by applying the general formula

$$\Psi = U_0 + \Psi_0 + \int_0^\lambda \langle \hat{V} \rangle_\lambda d\lambda, \qquad (4)$$

where $\lambda\hat{V}$ represents the Hamiltonian corresponding to the anharmonicity contribution. Then the free energy of the system is given by

$$\Psi = U_0 + 3N\theta\left[x + \ln\left(1 - e^{-2x}\right)\right] + 3N\left\{\frac{\theta^2}{k^2}\left[\gamma_2 x^2 \coth^2 x - \frac{2}{3}\gamma_1\left(1 + \frac{x\coth x}{2}\right)\right],\right.$$
$$\left. + \frac{2\theta^3}{k^4}\left[\frac{4}{3}\gamma_2^2 x\coth x\left(1 + \frac{x\coth x}{2}\right) - 2\gamma_1(\gamma_1 + 2\gamma_2)\left(1 + \frac{x\coth x}{2}\right)(1 + x\coth x)\right]\right\}$$
$$(5)$$

where the second term denotes the harmonic contribution to the free energy. With the aid of the "real space" free energy formula $\Psi = E - TS$, one can find the thermodynamic quantities of given systems (including nanoscale materials). The thermodynamic quantities such as specific heats and elastic moduli at temperature T are directly derived from the free energy Ψ of the system. The specific heat at constant pressure C_P, the adiabatic compressibility χ_S, and isothermal bulk modulus B_T are determined from the well known thermodynamic relations

$$C_P = C_V + \frac{9TV\alpha^2}{\chi_T}, \quad \chi_S = \frac{C_V}{C_P}\chi_T, \text{ and } B_T = \frac{1}{\chi_T} \qquad (6)$$

3. RESULTS AND DISCUSSIONS

Recently, the extensive experimental and theoretical studies have been done for the mechanical properties of carbon nanotubes (CNT) and the related nanomaterials and some specific informations on the dislocation nucleation and plastic flows have been demonstrated [2]. For instance, in the strained nanotubes at high temperatures one observe the spontaneous formation of double pentagon-heptagon defect pairs [26-28].

3.1. Thermodynamic quantities

We have calculated the thermal expansion coefficients and Young's moduli of CNTs as a function of the temperature T. We have found that the thermal expansions and elastic properties depend strongly on the chirality of CNT. It is interesting to note that the Young's moduli of CNT containing dislocations (characterized by 5/7 defects), dot-dashed lines, are smaller than those containing no dislocations and Stone-Wales (SW) defects. We have also calculated the specific heats C_v at constant volume of CNTs, as a function of the temperature [11,12]. The calculated C_v values of CNTs are given in unit of the Boltzmann constant k_B, and compared with those of the bulk materials. It has been found that the calculated specific heats $C_v(k_B)$ depend sensitively on the type of CNTs, except for the (6,6) CNT, having very similar temperature dependence to the diamond cubic crystal.

3.2. SW defects and nucreation of micro cracks

In the present article, we will study the properties of double ended cracks in the nanoscale crystallites. We have calculated the atomic configurations around the crack tips in the graphen sheets as well as in CNTs, using the constraint molecular dynamics combined with the lattice Green's function (LGF) method. In these calculations, the small double ended cracks are introduced by annihilating the interatomic bonds across the cleavage plane both for the c-MD and LGF treatments.

Firstly, we calculate the formation energies of the SW defects in the graphen in the application of the tensile

strain. The calculated formation energies are compared with those values in CNT. We have obtained the negative values in the tensile strain as in the case of CNT. In this respect, we note that, in the strained nanotubes at high temperatures one observe the spontaneous formation of double pentagon-heptagon defect pairs [26-28]. We have found that the transverse arrays of SW defects is the most stable compared to those of the vertical and 45° declined arrays [13]. The present results thus give the important information on the accumulations of the dislocations and Stone-Wales defects.

We have also studied the crack opening processes initiating from the smallest bond breaking defects as well as from SW defects in graphen sheets using the c-MD method. The micro cracks initiated in the core region of the SW defects open under mode I loading (tensile strain of ~0.1) and the bond breaking processes at the initial MD stage. We have found that the further slight increase of the mode I loading does not extend the cracks, and the crack length remains constant. In other words, quite large lattice trapping occurs for this type of "impotent" micro cracks. Therefore, in order to extend the micro crack it is necessary to accumulate further the SW defects in the crack plane. On the other hand, the cracks initiated from the smallest bond breaking defects propagate more easily than those initiated from the SW defects.

We have studied using c-MD method, the initiation and propagation of the micro-cracks in the CNTs originated from the SW defects as well as those from the bond breaking defects. The atomic configurations of the CNTs including SW defects, i.e., a pair of 5/7 defects, 5/7/8/7/5 and 5/7/8/8/7/5 type are calculated. We have also calculated the atomistic configurations of the double ended cracks initiated from SW defects (5/7/8/8/7/5 type) in (10,10) CNT, slightly lower than the critical tensile strain. We have found that the double ended cracks is clearly trapped in the "lattice" of (10,10) CNT. For comparison, we have also calculated the crack propagations and fracture of (10,10) CNT, calculated under the mode I tensile loadings considerably higher than the critical ("Grifith") strain of $\varepsilon_c \sim 0.12$. We have further calculated the atomic configurations of the (10,10) CNTs, including the double ended cracks, initiated from the 5/7/8/8/7/5 type of SW defects under the sufficiently high external loadings. Here, we can observe the CNTs are broken into two pieces, after the sufficient MD simulations.

Finally, we have calculated the atomic configurations of the double ended cracks in the cleavage plane of the 2D graphen sheets, under applied tensile stresses. In this calculation, we have assumed that the certain bonds across the cleavage plane are broken at the initial stage of MD relaxation processes. After the sufficient MD simulations, however, no assumptions on the bond breakings are made for the whole crystallites. This is a spirit of our constraint MD scheme. Using such MD procedure, one can get the stable equilibrium cracks in the small crystallites, which are essentially the similar results as those obtained by the analytic LGF method. As in the infinite three dimensional crystals, the double ended cracks are trapped in the small crystallites at certain mode I loadings. However, upon the increase of

the mode I loading to some extent, the micro cracks do extend, by one atomic distance, to the next stable positions. This is in marked difference to those of the "impotent" non-propagating cracks in the previous subsections.

For the calculations of the double ended cracks in the graphen sheets, slightly higher than the critical "Grifith" tensile loadings, we have found that the double ended cracks propagate to both surfaces of the graphens and the "specimen" separates into two spices. We have checked the "strain energies" releasing rates for every 10 MD steps and found that the strain energies of graphen sheets including the cleavage crack are reduced rapidly at the initials stage of the MD processes. Here, it is important to note that the surface excess energies γ due to the cleaved surface in the crystallites are approximately constant during the initial stage of the c-MD calculations, even when the crack opening displacements are nearly zero, since the "bond annihilation" operations are active from the beginning of the calculations. This is one of the advantages of the c-MD approach in the analysis of crack problems. From the middle to the final stages of c-MD simulations, the reduction of strain energies corresponds to the changes in the elastic and surface energies.

3.4. Conductivity of SWCNT with defects

We consider the case of a finite length single wall carbon nanotubes (SWCNT) connected at both ends to semi-infinite metallic leads [29]. The most commonly used computational schemes for calculating the electronic current in a SWCNT in contact with metal leads is based on the Landauer expression which relates the electron conduction G, with the transmission function $T(E)$, obtained using either the transfer Hamiltonian approach or the Green's function scattering formalism. We will use the Green's function approach coupled with a simple tight-binding model with one π -electron per atom [30-32] in the present calculations, to see the effects of crack like defects on the conductivity. We examine the local density of states in various sides in the CNT including defects and cracks. Our π -electron tight-binding Hamiltonian is of the form

$$H = -V_{pp\pi}\sum_{i>j}C_i^+ C_j^{'} + C.C. \qquad (7)$$

This type of simple model can give a reasonable qualitative description of the electronic and transport properties of an ideal CNT, through the connectivity of the atoms. In this model, the intratublar interactions are restricted to electron hopping between nearest-neighbour atoms only. The values of the hopping integral t_{ij} is described by a simple exponential relation to the C-C bond length R_{ij} as

$$t_{ij} = t_0 e^{-\alpha(R_{ij}-R_0)}, \qquad (8)$$

where R_0 is the reference bond length, which is fixed to 1.40Å for the CNT's considered here. The

parameters α and t_0 are taken to be $\alpha = 2.0\text{Å}^{-1}$ and $t_0 = -2.5eV$, respectively.

Transition through SWNT's involves the coupling between the metal contacts R and L and the conductor (tube) C as well as the transport along the conductor molecules. The transmission function $T(E)$ can be expressed in terms of the Green's functions of the conductors and the coupling of the conductor to the leads as

$$T(E) = Tr\left(\Gamma_L G_C^r \Gamma_R G_C^a\right), \qquad (9)$$

where G_C^r and G_C^a are the retarded and advanced Green's functions of the conductor C, respectively. Γ_L and Γ_R represent the coupling functions between the conductor C and the leads L and R, respectively. Here, the focus is on the changes in the properties of CNT. Therefore, the metal contacts are described in a simple way by cubic tight-binding lattices [32]. The lattice properties are described by a lattice parameter a (2.8Å simulating the lattice constant of gold), hopping $t_i(=-2.5eV)$ and onsite energy $\varepsilon_i(=0eV)$. (For more realistic calculations, it would be necessary to use of full orbital basis sets, as treated in the Green's function embedding approach [33,34]).

Fig.2 Initiation of a micro crack from SW defects in (10,10) CNT.

Fig.3 Crack propagations initiated from SW defects (a~c) and those from vacancy type defects (d~f) in (10,10) CNT.
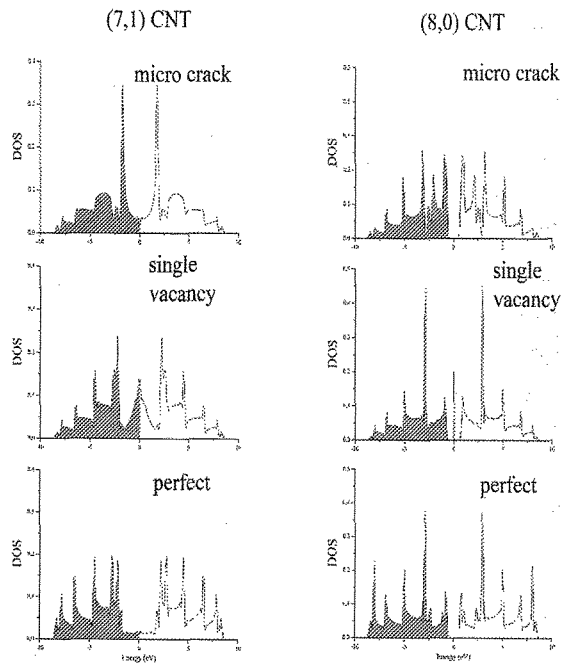

Fig.1 Comparisons of DOS between perfect and defected tubes

In Fig.1, we present the local electronic density of states for (7,1) and (8,0) CNTs, with and without lattice defects. One can see in Fig.1 that there are marked differences in the local DOS for atoms near the micro cracks (single bond broken) and vacancy defects.

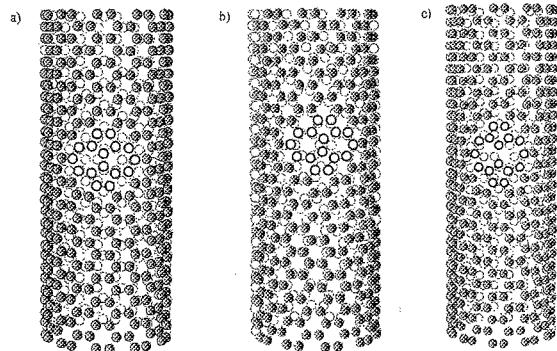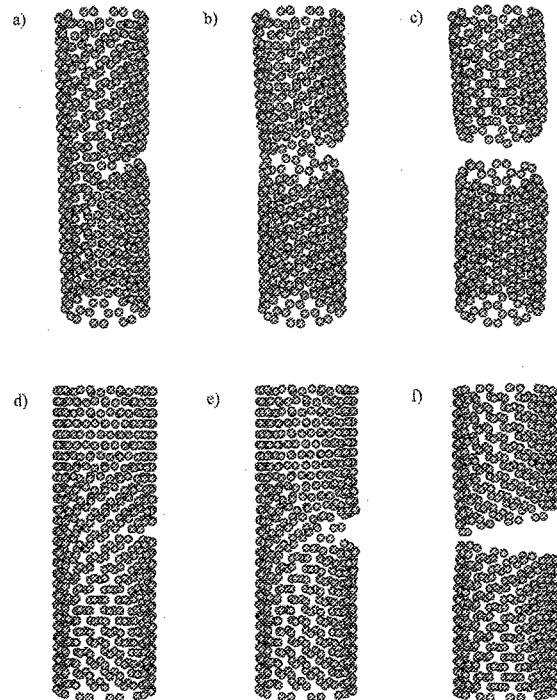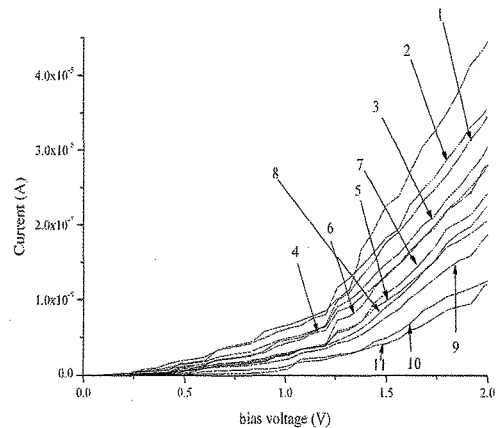In Fig.2, we present the initiation of micro cracks from SW defects in (10,10) carbon nanotubes:

Fig.4 Electric current (A) versus applied voltage (V) for (6,6) CNT with micro cracks.

The propagations of the micro cracks from SW defects

are shown in Figs.3a~3c. The propagations of micro cracks initiated from vacancy defects are presented in Figs.3d~3f. We have found that the propagation of the micro crack depends sensitively on the initial atomic configuration of the nucleated cracks.

Figure 4 shows the quantum currents versus applied bias voltage for (6,6) CNT with micro cracks: the numbers of broken bonds in the microcracks are 1~11.

In the present calculations, we have found that the shape of the I-V (current versus voltage) characteristic is sensitive to the presence of the atomic defects like SW defects, as well as the crack like "bond breaking" defects, the latter are more prominent than the former ones. This indicates that the electric conductivity measurement is one of the suitable "tools" for the "non-destructive" inspections" of the fracture of CNTs related functional nanostructures and the related devices.

4. Conclusions

We have employed a minimal parameter ab initio TBMD scheme and investigated the properties of atomic defects like SW defects and cracks in the nanoscale materials, i.e., quasi-1D and 2D carbon related materials. In the analysis of the crack opening and extension events, we have introduced the new constraint Molecular Dynamics (c-MD) method. It has been shown that there are two kinds of cracks in the nanoscale materials, i. e., strongly lattice trapped "impotent" cracks and the propagating cleavage cracks under the modest external loadings. The thermodynamic quantities of nanoscale materials like thermal expansions, specific heats, elastic constants, Grüneisen constants are calculated by using the SMM as a function of the temperature. We have found that the thermodynamic and electronic properties of nanoscale materials depend sensitively on their geometrical structures and different from those of the bulk materials.

References

[1] J. P. Hirth and J. Lothe, "Theory of Dislocations", (Wiley, New York, 1982).

[2] "Trends in Nanoscale Mechanics", ed. By V. M. Harik and M. D. Salas, (Kluwer Academic Publishers, 2003).

[3] "Nanoscale Materials", ed. By L. M. Liz-Marzán and P. V. Kamlat, (Liuwer Academic, 2003).

[4] "Semiconductor Nanocrystals", ed. By D. J. Lockwood, (Kluwer Academic/Plenum, 2003).

[5] S. Iijima, Nature 354 (1991) 56.

[6] K. Masuda-Jindo and R. Kikuchi, Int. J. of Nanoscience, 1, (2002) 357-371.

[7] A. Hansson, M. Paulsson and S. Stafström, Phys. Rev. B62, (2000) 7639.

[8] A. J. Lu and B. C. Pan, Phys. Rev. Lett., 92 (2004) 105504.

[9] P. Ordejon, D. Lebedenko and M. Menon, Phys. Rev. B50 (1994) 5645.

[10] M. Menon, E. Richter and K. R. Subbaswamy, J.Chem.Phys. 104,(1996) 5875

[11] K. Masuda-Jindo and Vu Van Hung, Physical Mesomechanics, Vol.7, No.4 (2004) 77.

[12] K. Masuda-Jindo, V. V. Hung and M. Menon, International Journal of Fracture 125, (2006) 1.

[13] K. Masuda-Jindo, Vu Van Hung and M. Menon, Phys. stat. sol. (c) 2, No. 6, (2005) 1781.

[14] K. Masuda-Jindo and Vu Van Hung, J. Phys. Soc. Jap. 73 (2004) 1205.

[15] T. J. Matsubara, J. Phys. Soc. Jpn., 7 (1952) 270.

[16] H. Kanzaki, J. Phys. Chem. Solids, 2 (1957) 24.

[17] V. K. Tewary, Adv. Phys. 22, (1973) 757.

[18] D. M. Esterling, J. Appl. Phys., 47 (1976) 486.

[19] K. Masuda-Jindo, V. K. Tewary and R. Thomson, J.Mater.Res., 2 (1987) 631.

[20] K. Masuda-Jindo, V. K. Tewary and R. Thomson, J.Mater.Res., 6(1991) 1553.

[21] V. K. Tewary and R. Thomson, J. Mater. Res., 7 (1992) 1018.

[22] V. K. Tewary, E. R. Fuller Jr. and R. M. Thomson, J.Mater.Res., 4 (1989) 309.

[23] V. V. Hung and K. Masuda-Jindo, J. Phys. Soc. Jap. 69 (2000) 2067.

[24] K. Masuda-Jindo, Vu Van Hung and Pham Dinh Tam, Phys. Rev. B67(2003) 094301.

[25] K. Masuda-Jindo, S. Nishitani and Vu Van Hung, Phys. Rev. B70(2004) 184122.

[26] M. B. Nardelli, B. I. Yakobson and J. Bernholc, Phys.Rev. B57,(1998) R4277.

[27] M. B. Nardelli, B. I. Yakobson and J. Bernholc, Phys.Rev.Lett.81,(1998) 4656.

[28] B. I. Yakobson, Appl. Phys. Lett., 72, (1998) 918.

[29] S. Datta, "Electronic Transport in Mesoscopic Systems", (Cambridge University press, Cambridge, 1995).

[30] M. P. Samanta, W. Tian, S. Datta, J. I. Henderson, and C. P. Kubiak, Phys. Rev. B53, (1996) R7626

[31] M. B. Nardelli, Phys. Rev. B60, (1999) 7828.

[32] A. Hansen, M. Paulsson and S. Stafström, Phys. Rev. B62, (2000) 7639

[33] N. Andriotis and M. Menon, J. Chem. Phys. 115, (2001) 2737

[34] A. N. Andiotis and M. Menon, "Complex Inorganic Solids", structural Stability and Magnetic Properties of Alloys, (Springer, 2002) P25A.